DOI: 10.1002/anie.201410987

Layered Compounds

β-CuN$_3$: The Overlooked Ground-State Polymorph of Copper Azide with Heterographene-Like Layers[**]

Xiaohui Liu, Janine George, Stefan Maintz, and Richard Dronskowski[*]

Dedicated to Professor Francis J. DiSalvo on the occasion of his 70th birthday

Abstract: *An unexpected polymorph of the highly energetic phase CuN$_3$ has been synthesized and crystallizes in the orthorhombic space group Cmcm with $a = 3.3635(7)$, $b = 10.669(2)$, $c = 5.5547(11)$ Å and $V = 199.34(7)$ Å^3. The layered structure resembles graphite with an interlayer distance of 2.777(1) Å ($= {}^1\!/_2\,c$). Within a single layer, considering N_3^- as one structural unit, there are 10-membered almost hexagonal rings with a heterographene-like motif. Copper and nitrogen atoms are covalently bonded with Cu–N bonds lengths of 1.91 and 2.00 Å, and the N_3^- group is linear but with N–N 1.14 and 1.20 Å. Electronic-structure calculations and experimental thermochemistry show that the new polymorph termed β-CuN$_3$ is more stable than the established α-CuN$_3$ phase. Also, β-CuN$_3$ is dynamically, and thus thermochemically, metastable according to the calculated phonon density of states. In addition, β-CuN$_3$ exhibits negative thermal expansion within the graphene-like layer.*

Nitrogen-rich materials, such as azides, have been and are still used as important and classical energetic materials.[1] Nonetheless, because of environmental issues and their critical instability (impact, friction, electrostatic and thermal sensitivity), heavy-metal azides are gradually being replaced by organic azides,[2] despite the fact that the very recent past has witnessed surprisingly new and ingenious soft-chemical routes to metal azides from liquid ammonia.[3] The established copper(I) azide, α-CuN$_3$, which is even more sensitive to heat and impact than the notorious Pb(N$_3$)$_2$, however, has apparently never been utilized as an energetic material.[4] There is a pioneering crystal-structure report from 1948[5] but since then chemists have clearly avoided performing more experiments on α-CuN$_3$, for understandable reasons. We have now synthesized an unexpected new polymorph of copper azide termed β-CuN$_3$ by a slightly modified route and, also, by an until now unknown phase transition of α-CuN$_3$ in aqueous solution. Owning to its unique graphite-like structure, we report herein its synthesis, thermochemical data, electronic-structure theory, phonon densities of states, chemical bonding, and mechanical properties.

The structure of α-CuN$_3$ can be simply described as a three-dimensional network of Cu$^{\mathrm{I}}$ and N_3^- groups oriented along the unit cell's body diagonal (Figure 1). The d^{10}-configured Cu$^{\mathrm{I}}$ experiences a distorted planar coordination by four N_3^- units, and vice versa (Figure 1), with 2 × Cu–N 2.23(1) and 2 × Cu–N 2.30(1) Å and a perfectly $D_{\infty h}$-symmetric azide ion with N–N 1.17(1) Å. The empirical bond-valence sum for Cu$^{\mathrm{I}}$ is thus rather small and a bit suspicious at 0.68.[6] It is clear from the literature that this phase has been regarded

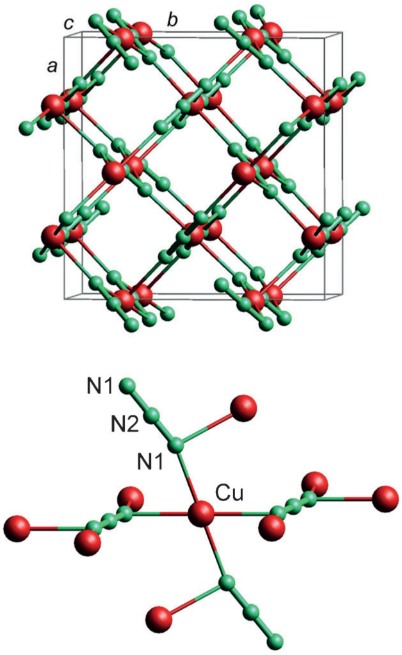

Figure 1. The known crystal structure of α-CuN$_3$ in which Cu$^{\mathrm{I}}$ atoms and N_3^- groups are arranged in chains along the unit cell's body diagonal (top). Each Cu$^{\mathrm{I}}$ is almost planarly surrounded by four nitrogen atoms from the N_3^- group, and vice versa (bottom).

---

[*] Dr. X. Liu, J. George, M. Sc. Dipl.-Chem. S. Maintz, Prof. Dr. R. Dronskowski
Institut für Anorganische Chemie, Lehrstuhl für Festkörper- und Quantenchemie, RWTH Aachen
Landoltweg 1, 52056 Aachen (Germany)
E-mail: drons@HAL9000.ac.rwth-aachen.de

Prof. Dr. R. Dronskowski
Jülich-Aachen Research Alliance (JARA-HPC), RWTH Aachen
52056 Aachen (Germany)

[**] This work was partially supported by DFG. We are very thankful to Prof. Ulli Englert for help in handling the data of the twin crystal, Dr. Paul Müller for the measurements of temperature-dependent powder XRD, Dr. Klaus Beckerle for the DSC measurements, as well as Volker Deringer for helpful remarks. We are also grateful for CPU time provided by the high-performance computing cluster at the IT Center of RWTH Aachen University (project: jara0069). J.G. thanks the Fonds der Chemischen Industrie for a Chemiefonds scholarship.

Supporting information for this article is available on the WWW under http://dx.doi.org/10.1002/anie.201410987.

as the ground state of CuN_3, and there have also been theoretical calculations validating its existence but without addressing the dynamic character in terms of phonons.[7] This situation is even more astonishing since some doubts about the correctness of this crystal structure had already been raised by Dehnicke in the mid 1970s based on vibrational spectra.[8] As will be clear from what follows, Dehnicke's doubts were justified.

Puzzlingly, the new ground-state phase of CuN_3 can be synthesized by almost the same procedure, and it is difficult to understand why it has been overlooked for such a long time.[5] Indeed, just a small improvement is needed to obtain the new β phase in pure form. To cautiously(!) synthesize α-CuN_3, Cu^{2+} is first reduced to Cu^+ by Na_2SO_3, then NaN_3 is added. After several minutes, careful filtering and washing leads to α-CuN_3. It is fascinating that by simply keeping α-CuN_3 in the mother solution, it will partly recrystallize into β-CuN_3 within days. For a more direct synthesis of β-CuN_3, a Cu^{II} salt and NaN_3 solution are mixed to form a brown precipitate, and adding Na_2SO_3 leads to a mixture of α- and β-CuN_3. After several hours, the entire precipitate consists of phase-pure β-CuN_3. α- and β-CuN_3 are easily distinguishable from X-ray powder diffraction data because they have strongly differing Bragg reflections (Supporting Information).

The crystal structure of β-CuN_3 as well as the coordination environments of both Cu^I and N_3^- ions are displayed in Figure 2. The structure is composed of infinite heterographene-like layers of Cu^I and N_3^- arranged in the form of perfectly planar 10-membered "hexagons". The stacking arrangement along *c* is *ABAB* with Cu^I and N_3^- ions in alternating planes aligning with each other, similar to graphite[9] and dissimilar to boron nitride.[10] The interlayer distance is 2.777(1) Å (that is, half the *c* axis) such that β-CuN_3 ($\rho = 3.52\,g\,cm^{-3}$) is about 8% more dense than α-CuN_3 ($3.26\,g\,cm^{-3}$).

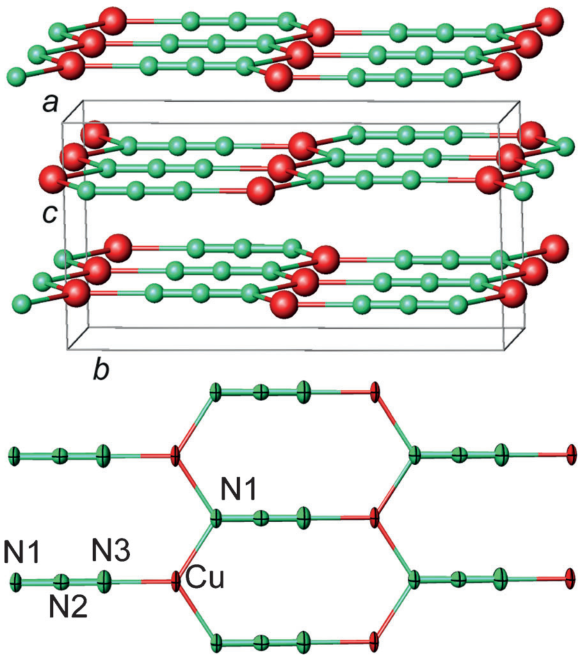

Figure 2. The crystal structure of β-CuN_3 adopting a graphite-like layered structure with an inter-layer distance of 2.78 Å (top) and the coordination of Cu^I within the layer drawn with thermal ellipsoids set at 90% probability (bottom).

The Cu^I coordination by the N_3^- corresponds to a slightly distorted but planar triangle with 2 × Cu–N 1.999(2) and 1 × Cu–N 1.910(4) Å. The short distances indicate a stronger covalent bonding than in α-CuN_3 and, consequently, Cu^I has a larger bond-valence sum of 1.14. Because the terminal nitrogen atoms bind to one Cu^I atom from one side and to two Cu^I atoms from the other side, the N_3^- group is still linear but conforms to $C_{\infty v}$ symmetry with N–N 1.140(6) and 1.203(6) Å. The relatively short interlayer Cu–Cu distance, 2.82(1) Å, is much larger than twice the effective ionic radius of Cu^I.[11] Although interactions with even longer Cu–Cu distances have been claimed,[12] such interactions are unlikely in nature at distances greater than 2.5 Å.[13]

For β-CuN_3, the lattice parameters and bond lengths derived at the PBE + D3/PAW level of theory, are in very good agreement with the experimental ones: $a = 3.351$, $b = 10.615$, $c = 5.516$ Å, Cu–N 1.867 and 1.986 Å (max. deviation $< 1\%$), N–N 1.165 and 1.208 Å, and Cu–Cu 2.796 Å (max. deviation $< 2.5\%$). The results of several other levels of theory are presented in the Supporting Information. Astonishingly at first sight, a related optimization for α-CuN_3 was impossible because a drastic structural change occurred during relaxation. In fact, the supposedly "stable" α-CuN_3 suffers from massive internal instabilities (see also below) such that all remaining calculations of α-CuN_3 were carried out on the basis of the experimental structure.[5] It is quite probable that the formerly reported structural optimization of α-CuN_3[7] did not lead to a local minimum of its Born–Oppenheimer potential hypersurface but got stuck somewhere else.

To investigate the thermochemical behavior of both phases, phonon density of states (DOS) were calculated. Although α-CuN_3 clearly exhibits plenty of imaginary modes (Figure 3), β-CuN_3 does not. Hence, β-CuN_3 is theoretically identified as the ground-state phase. Likewise, it is almost miraculous that α-CuN_3 crystals can indeed be subjected to structural analysis given the electronic-structure finding that the phase decays into β-CuN_3 at any temperature. If such transformation (α→β) was also present in Dehnicke's studies,[8] the discrepancies between crystal structure and spectroscopy are immediately explained.

To probe the optical properties, the electronic densities of states for both structures (α and β) were calculated at a high level of theory based on the experimental structures. HSE06 predicts α-CuN_3 to reveal a band gap of 3.4 eV which is not far away from an earlier but more simple (LDA) calculation yielding 2.6 eV.[7b] β-CuN_3 should have a narrower band gap of 2.4 eV, and that surprising result agrees with the slightly gray appearance of the crystals so that β-CuN_3 can absorb electromagnetic radiation of the visible spectrum. Hence, theory corroborates the unexpected experimental result of a smaller band gap for the more stable polymorph.

The enthalpy difference between α- and β-CuN_3 should show up in differential scanning calorimetric (DSC) measurements. As expected, both compounds start to decompose very energetically to Cu metal and nitrogen gas above 150 °C, with

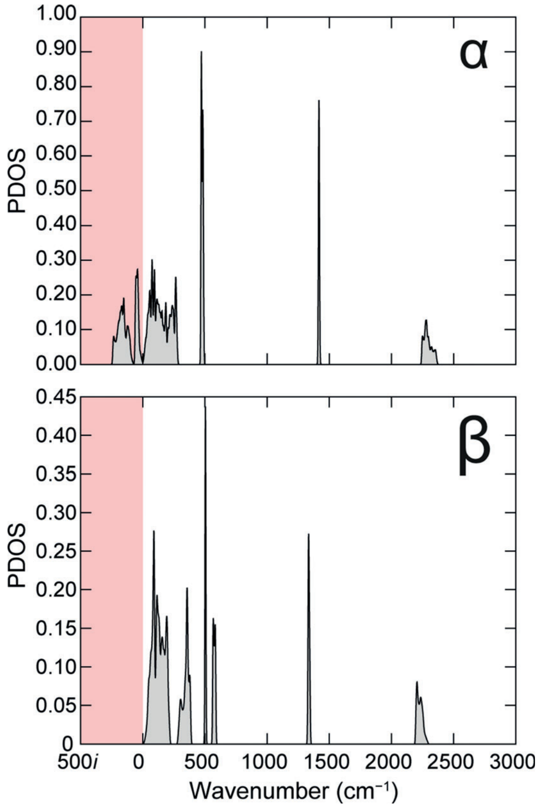

Figure 3. Phonon DOS (PDOS) of α-CuN_3 (top) and β-CuN_3 (bottom). While the PDOS of α-CuN_3 exhibits imaginary modes, that of β-CuN_3 does not, thereby indicating dynamic metastability.

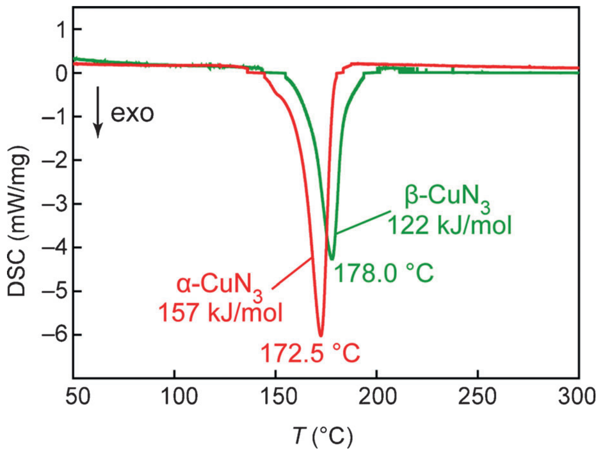

Figure 4. DSC measurements on α- and β-CuN_3 performed under N_2 atmosphere. Both compounds start to decompose above 150 °C.

excess enthalpies of 157 kJ mol^{-1} for α-CuN_3 and 122 kJ mol^{-1} for β-CuN_3 (Figure 4). Surprisingly and luckily enough, under the DSC conditions and protective N_2 atmosphere, the energy release occurs over a temperature range of 50 °C for one hour and not by explosion. Hence, the behavior is quite different to the DSC measurements of explosive PbN_3Cl for which a very sharp peak was observed.[14]

To gain more insight into the electronic reason for the different stabilities of α- and β-CuN_3, projected crystal orbital Hamilton populations[15] (pCOHPs) were calculated, and we concentrate on the shortest Cu–N bonds in both compounds (Figure 5), namely the four Cu–N ≤ 2.3 Å in α-CuN_3 and the three Cu–N ≤ 2.0 Å in β-CuN_3. Both kinds of Cu–N interaction show occupied antibonding states below the Fermi level, reflecting an unfortunate bonding situation in both cases; we recall that both phases are explosives. Nevertheless, the Cu–N dispersion in the case of β-CuN_3 is wider and, therefore, these three shorter bonds are also more covalent. The visual inspection also reveals that the Cu–N bonds in β-CuN_3 are more than twice as strong than in α-CuN_3, at least in terms of the band-structure energy, thereby corroborating the earlier bond-valence argument. There is good reason to believe that the source of the imaginary phonon frequencies and structural instability of α-CuN_3 seems to stem from its relatively weak Cu–N interactions. Again, the existence of α-CuN_3 must be considered as good fortune for structure determination.

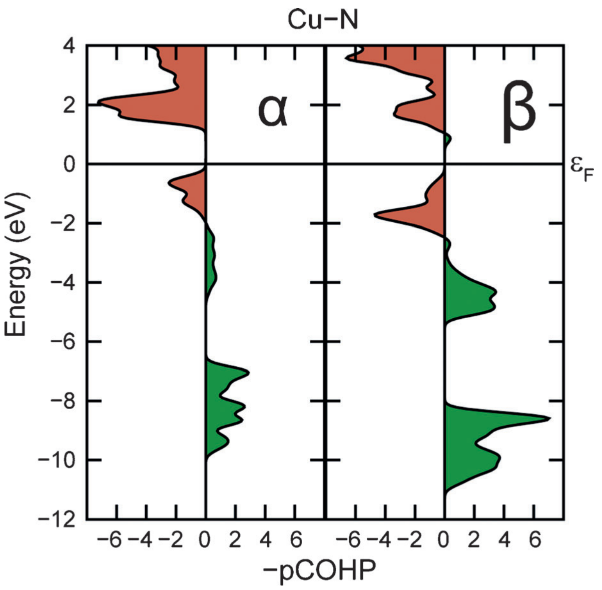

Figure 5. Projected COHP curves of the shortest Cu–N interactions in α-CuN_3 (2×2.23 and 2×2.30 Å, left) and β-CuN_3 (1×1.91 Å, 2×2.00, right) based on the PBE functional.

Eventually, the perplexing structure of β-CuN_3 suggests unconventional, anisotropic mechanical properties, and this expectation is indeed reflected from the thermal-expansion coefficients which were determined in the range 50–290 K based on X-ray powder-diffraction patterns (Supporting Information). The linear thermal-expansion coefficient can be written as $\alpha_L = (1/L)(\mathrm{d}L/\mathrm{d}T)$, where L is a particular length measured at room temperature (in this case: 290 K).

Upon heating, only the lattice parameter c increases whereas a and b clearly decrease (Figure 6); the overall volume, however, also increases slightly while the temperature increases. The temperature dependence of the lattice parameters not only differs by their signs but also by their magnitude. The shrinkage of a and b and the expansion of c, respectively, occur almost linearly with slopes of $-5.2(3)\times 10^{-5}$ Å K^{-1}, $-2.38(6)\times 10^{-4}$ Å K^{-1}, and $+5.05(7)\times 10^{-4}$ Å K^{-1}. This results in thermal coefficients of $-15.4(8)\times 10^{-6}$ K^{-1},

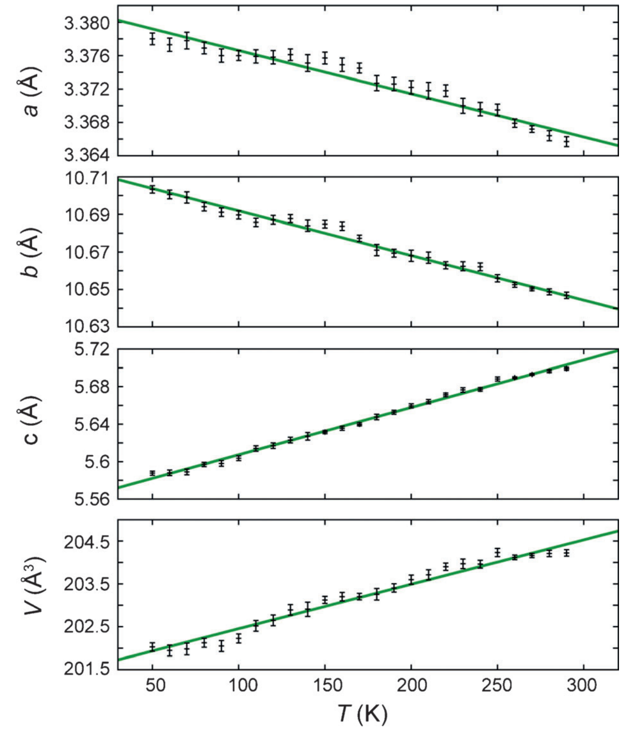

Figure 6. Change of the lattice parameters and volume of β-CuN_3 measured by temperature-dependent powder XRD between 50 and 290 K. The error bars indicate the standard deviation of the lattice parameters and volume, respectively.

$-22.4(6) \times 10^{-6}$ K^{-1}, and $+89(1) \times 10^{-6}$ K^{-1} along *a*, *b*, and *c*, respectively.

Looking at the crystal structure (Figure 2), we recall that the Cu–N bonds are found in the *ab* plane while the covalent N–N bonds are aligned along *b*, and the heterographene-like layers are stacked along *c*. The supposedly weak stacking interaction is clearly reflected in the expansion of *c* upon heating. Similar layered structures, such as graphite,[9] boron nitride[10] and, especially, the recently examined bromomalonic aldehyde[16] also show a large thermal expansion along such stacked layers, namely 40.5×10^{-6} K^{-1}, 28.3×10^{-6} K^{-1}, and 138×10^{-6} K^{-1}, respectively. Thus, the expansion of β-CuN_3 along *c* is more than twice as large when compared to the structurally closest species, graphite and boron nitride. Just like in graphite, β-CuN_3 exhibits a negative thermal expansion (NTE) solely within *ab*. The smallest change of the lattice parameter occurs along *a* where the covalent and rigid N–N bonds lie.

There are multiple structural reasons for the occurrence of NTE[17] including so-called "supramolecular" mechanisms.[18] Such effects may be related to increased vibrations perpendicular to the contracting, covalent chains and along the direction of weak van-der-Waals bonding (polyethylene).[19] Also, there are librations[15] and rotations of building blocks (ZrW_2O_8).[20] The ORTEP plots (Figure 2, bottom) of β-CuN_3 already reveal enlarged anisotropic displacement parameters of the terminal N1 and N3 atoms in the azide units, indicative of the aforementioned libration and other vibrations. In fact, a "riding" model of the azide unit around the central N2 atom based on the anisotropic thermal parameters yields rigid-body-corrected N1–N2 and N2–N3 distances of 1.207 and 1.149 Å.

In summary, β-CuN_3 was synthesized in phase-pure form, and its graphite-like crystal structure, energetics, and NTE behavior were experimentally determined. In addition, electronic-structure theory corroborates the finding that β-CuN_3 is the ground-state copper azide that has been overlooked for many decades.

Experimental Section

CAUTION: all heavy-metal azides are potential explosives! α-CuN_3: $CuCl_2 \cdot 2H_2O$ (0.34 g, 2 mmol) was dissolved in water (10 mL) in a round flask under inert gas, adding (0.25 g, 2 mmol) Na_2SO_3 in water (10 mL) gave a precipitate of CuCl (2 mmol). A one-fold excess of Na_2SO_3 ensured full reduction and rise of the pH value to the neutral range. Then, NaN_3 (0.13 g, 2 mmol) in water (5 mL) was added. Soon, a snow-white precipitate of α-CuN_3 was obtained. If α-CuN_3 is kept in the mother solution under inert gas for several days, the compound partly transforms to gray β-CuN_3.

Phase-pure β-CuN_3 was made by a modified route. First, a Cu^{II} salt solution was mixed with a molar equivalent NaN_3 solution, and a brown slimy precipitate was observed. Then, 4/3 molar mass of Na_2SO_3 in solution was slowly added to the mixture under inert gas. A mixed precipitate consisting of α- and β-CuN_3 was observed. After several hours stirring, phase-pure β-CuN_3 was obtained. Crystals of β-CuN_3 are gray and transparent, thus clearly different from those of α-CuN_3. The modified route ensures that the phase transition from α- to β-CuN_3 is more efficient. The inverse phase transition was never observed. The preferred crystallization of the more energetic α-phase may be easily interpreted in terms of Ostwald's step rule.

The products were analyzed by elemental analysis of H and N, atomic absorption spectroscopy (AAS) analysis of copper, as well as powder X-ray diffraction (G670 Imageplate Guinier diffractometer) for phase purity and phase transition.

A prismatic crystal of β-CuN_3 was fixed on a glass fiber in air. Intensity data were collected at 100(2) K using a Bruker SMART APEX CCD diffractometer with monochromatic $Mo_{K\alpha}$ radiation. Data collection and reduction were carried out with APEX2,[21] and the crystal was identified as a non-merohedral twin. An empirical absorption correction was performed with TWINABS. The structure was solved by direct methods using SHELXS and refined by full-matrix least-squares techniques based on intensities with the SHELXL program.[22] To correctly treat the itensities of the non-merohedral twin, the reflection file was modified using the HKLF 5 option so that equivalent reflections were not merged. The final refinement included the ratio of the two components and arrived at BASF = 0.112(9). All atoms were refined anisotropically. The rigid-body correction was carried out with the RIDE command in the XP routine.

Crystal data of β-CuN_3: $M_r = 105.57$, space group *Cmcm* (no. 63); $a = 3.3635(7)$, $b = 10.669(2)$, $c = 5.5547(11)$ Å and $V = 199.34(7)$ $Å^3$, $Z = 4$; $R_1[I > 2\sigma(I)] = 0.025$, $wR(I) = 0.055$; all atoms on 4*c* position ($x \equiv 0$, $z \equiv {}^1/_4$) with $y = 0.02371(3)$ for Cu, 0.4224(3) for N1, 0.3096(4) for N2 and 0.2027(3) for N3. Further details on the crystal structure investigations may be obtained from the Fachinformationszentrum Karlsruhe, 76344 Eggenstein-Leopoldshafen, Germany (fax: (+49) 7247-808-666; e-mail: crysdata@fiz-karlsruhe.de), on quoting the depository number CSD-428038 for CuN_3.

Differential scanning calorimetric (DSC) measurements were conducted with a NETZSCH DSC 204 instrument. The measurements of α-CuN_3 (0.70 mg) and β-CuN_3 (0.80 mg) were carried out under protective N_2 gas between 20–300 °C. The temperature was slowly increased by 1 K min^{-1}.

Powder XRD data for further temperature-resolved studies were collected with a G645 Guinier diffractometer (Huber, Rimsting) equipped with a closed-cycle Helium refrigerator using a linear position-sensitive detector (PSD, Stoe) in range of 14–60°. The temperature was varied between 50 and 290 K in steps around 10 K, summing up to 25 diffraction patterns. Finally, all 25 patterns were subsequently indexed in the WinXPow software package.[23] The cell refinements included the positions of the assigned reflections with a fixed zero point.

Theoretical Section

Density-functional calculations were carried out with the Vienna ab initio simulation package (VASP).[24] To do so, the GGA functional of Perdew, Burke, and Enzerhof (PBE)[25] and the projector augmented-wave method (PAW)[26] were applied. The kinetic energy cutoff of the plane-wave expansion was 500 eV. Owing to the clear relevance of van-der-Waals forces in layered β-$\mathrm{CuN_3}$,[27] several dispersion corrections were applied such as “D2”,[28] “D3”[29] with zero-damping and “D3(BJ)”[29,30] with the Becke-Johnson damping function, all as implemented in VASP 5.3.5. Especially the results of the “D3(BJ)” correction promise a very good agreement with experimental unit cell volumes and cohesive energies in the case of molecular crystals.[31] The “D2” correction has already proven success in the calculation of layered structures[28b] while the “D3”/“D3(BJ)” corrections are generally expected to be even superior. Such dispersion forces have recently become decisive in explaining the relative energetics of elemental phosphorus.[32] All atoms of β-$\mathrm{CuN_3}$ and the cell volume were fully relaxed until the Hellmann–Feynman forces were smaller than 5×10^{-3} eV Å^{-1}. Such a relaxation, however, was impossible for α-$\mathrm{CuN_3}$ since a drastic structural change occurred during this relaxation. Therefore, all aforementioned α-$\mathrm{CuN_3}$ calculations were carried out with the experimental structure. To our knowledge, only one “geometry relaxation” of α-$\mathrm{CuN_3}$ has been reported,[7a] and the structure was energetically converged using the PW91 functional. For all electronic structures, a convergence criterion of 10^{-6} eV was used.

The phonon densities of states were calculated according to the direct method.[33] The forces were calculated with VASP using a super-cell expansion of $2\times2\times3$ (α-$\mathrm{CuN_3}$; PBE + D3 level of theory based on the experimental structure) and $3\times1\times2$ (β-$\mathrm{CuN_3}$; PBE + D3 level of theory), respectively. The k-points for the prior optimization of β-$\mathrm{CuN_3}$ were $7\times3\times6$. The phonon DOS were calculated with $20\times20\times20$ and $63\times27\times54$ k-points, respectively, in PHONOPY. The k-points during the force calculations were $1\times1\times1$ and $3\times3\times3$, respectively. The convergence criterion for the structure optimization was 10^{-5} eV, and that for the electronic structure was 10^{-7} eV.

The projected crystal orbital Hamilton populations[15,34] (pCOHPs) were derived from the LOBSTER program suite for electronic-structure reconstruction based on the VASP result calculated at PBE level of theory using the experimental structures. The standard Cu basis set[35] as implemented in LOBSTER was augmented with a virtual 4p orbital fitted to corresponding free-atom PAW wave functions to reduce charge spilling to 0.35 and 0.15 % for α- and β-$\mathrm{CuN_3}$, respectively. The Hamiltonian was reconstructed by an improved scheme explicitly including the overlap matrix.

The shortcomings of typical DFT functionals concerning band gaps are well documented.[36] Therefore, the electronic structure was recalculated using VASP at the HSE06/PAW level of theory on the basis of the experimental structures and employing the tetrahedron method.[37] This level of theory was used since the Heyd–Scuseria–Ernzerhof functional is one attempt to obtain accurate band gaps and band structures for—at least—bulk semiconductors.[38] The kinetic energy cutoff of the plane-wave expansion was 400 eV.

Received: November 12, 2014

Keywords: azides · density functional calculations · electronic structure · phase transitions · thermochemistry

---

[1] a) T. M. Klapötke, N. Mehta, *Propellants Explos. Pyrotech.* **2014**, *39*, 7–8; b) G. Steinhauser, T. M. Klapötke, *Angew. Chem. Int. Ed.* **2008**, *47*, 3330–3347; *Angew. Chem.* **2008**, *120*, 3376–3394.
[2] J. Köhler, R. Meyer, A. Homburg, *Explosivstoffe*, Wiley-VCH, Weinheim, **2008**.
[3] T. G. Müller, F. Karau, W. Schnick, F. Kraus, *Angew. Chem. Int. Ed.* **2014**, *53*, 13695–13697; *Angew. Chem.* **2014**, *126*, 13913–13915.
[4] K. Singh, *Trans. Faraday Soc.* **1959**, *55*, 124–129.
[5] H. Wilsdorf, *Acta Crystallogr.* **1948**, *1*, 115–118.
[6] N. Brese, M. O’Keeffe, *Acta Crystallogr. Sect. B* **1991**, *47*, 192–197.
[7] a) W. Zhu, H. Xiao, *J. Comput. Chem.* **2008**, *29*, 176–184; b) A. Gordienko, A. Poplavnoĭ, *Phys. Solid State* **2006**, *48*, 1844–1847.
[8] K. Dehnicke, *Z. Anorg. Allg. Chem.* **1974**, *409*, 311–319.
[9] A. W. Hull, *Phys. Rev.* **1917**, *10*, 661–696.
[10] R. Pease, *Acta Crystallogr.* **1952**, *5*, 356–361.
[11] R. Shannon, *Acta Crystallogr. Sect. A* **1976**, *32*, 751–767.
[12] J. Zuo, M. Kim, M. O’Keeffe, J. Spence, *Nature* **1999**, *401*, 49–52.
[13] S.-G. Wang, W. H. E. Schwarz, *Angew. Chem. Int. Ed.* **2000**, *39*, 1757–1762; *Angew. Chem.* **2000**, *112*, 1827–1832.
[14] X. Liu, R. Stoffel, R. Dronskowski, unpublished results.
[15] R. Dronskowski, P. E. Blöchl, *J. Phys. Chem.* **1993**, *97*, 8617–8624.
[16] V. L. Deringer, F. Pan, J. George, P. Müller, R. Dronskowski, U. Englert, *CrystEngComm* **2014**, *16*, 135–138.
[17] S. Haas, B. Batlogg, C. Besnard, M. Schiltz, C. Kloc, T. Siegrist, *Phys. Rev. B* **2007**, *76*, 205203.
[18] W. Miller, C. W. Smith, D. S. Mackenzie, K. E. Evans, *J. Mater. Sci.* **2009**, *44*, 5441–5451.
[19] a) J. A. O. Bruno, N. L. Allan, T. H. K. Barron, A. D. Turner, *Phys. Rev. B* **1998**, *58*, 8416–8427; b) G. D. Barrera, J. A. O. Bruno, T. H. K. Barron, N. L. Allan, *J. Phys. Condens. Matter* **2005**, *17*, R217.
[20] Y. Sato, Y. Yamamura, K. Saito, Y. Ikuhara, *J. Am. Chem. Soc.* **2012**, *134*, 13942–13945.
[21] Bruker APEX2; Bruker AXS Inc., Madison, WI, **2005**.
[22] G. Sheldrick, *Acta Crystallogr. Sect. A* **2008**, *64*, 112–122.
[23] WinXPOW version 1.06 STOE & CIE GmbH, **1999**.
[24] a) G. Kresse, J. Hafner, *Phys. Rev. B* **1993**, *47*, 558–561; b) G. Kresse, J. Hafner, *Phys. Rev. B* **1994**, *49*, 14251–14269; c) G. Kresse, J. Furthmüller, *Phys. Rev. B* **1996**, *54*, 11169–11186; d) G. Kresse, J. Furthmüller, *Comput. Mater. Sci.* **1996**, *6*, 15–50.
[25] J. P. Perdew, K. Burke, M. Ernzerhof, *Phys. Rev. Lett.* **1996**, *77*, 3865–3868.
[26] a) P. E. Blöchl, *Phys. Rev. B* **1994**, *50*, 17953–17979; b) G. Kresse, D. Joubert, *Phys. Rev. B* **1999**, *59*, 1758–1775.
[27] D. Tunega, T. Bučko, A. Zaoui, *J. Chem. Phys.* **2012**, *137*, 114105.
[28] a) S. Grimme, *J. Comput. Chem.* **2006**, *27*, 1787–1799; b) T. Bučko, J. Hafner, S. Lebègue, J. G. Ángyán, *J. Phys. Chem. A* **2010**, *114*, 11814–11824.
[29] S. Grimme, J. Antony, S. Ehrlich, H. Krieg, *J. Chem. Phys.* **2010**, *132*, 154104.
[30] S. Grimme, S. Ehrlich, L. Goerigk, *J. Comput. Chem.* **2011**, *32*, 1456–1465.
[31] J. Moellmann, S. Grimme, *J. Phys. Chem. C* **2014**, *118*, 7615–7621.
[32] F. Bachhuber, J. von Appen, R. Dronskowski, P. Schmidt, T. Nilges, A. Pfitzner, R. Weihrich, *Angew. Chem. Int. Ed.* **2014**, *53*, 11629–11633; *Angew. Chem.* **2014**, *126*, 11813–11817.
[33] a) K. Parlinski, Z. Q. Li, Y. Kawazoe, *Phys. Rev. Lett.* **1997**, *78*, 4063–4066; b) A. Togo, F. Oba, I. Tanaka, *Phys. Rev. B* **2008**, *78*, 134106.

[34] a) V. L. Deringer, A. L. Tchougréeff, R. Dronskowski, *J. Phys. Chem. A* **2011**, *115*, 5461 – 5466; b) S. Maintz, V. L. Deringer, A. L. Tchougréeff, R. Dronskowski, *J. Comput. Chem.* **2013**, *34*, 2557 – 2567; see also http://www.cohp.de.

[35] a) T. Koga, K. Kanayama, S. Watanabe, A. J. Thakkar, *Int. J. Quantum Chem.* **1999**, *71*, 491 – 497; b) T. Koga, K. Kanayama, T. Watanabe, T. Imai, A. J. Thakkar, *Theor. Chem. Acc.* **2000**, *104*, 411 – 413.

[36] a) J. P. Perdew, M. Levy, *Phys. Rev. Lett.* **1983**, *51*, 1884 – 1887; b) L. J. Sham, M. Schlüter, *Phys. Rev. Lett.* **1983**, *51*, 1888 – 1891.

[37] P. E. Blöchl, O. Jepsen, O. K. Andersen, *Phys. Rev. B* **1994**, *49*, 16223.

[38] M. Jain, J. R. Chelikowsky, S. G. Louie, *Phys. Rev. Lett.* **2011**, *107*, 216806.